Calhoun: The NPS Institutional Archive
DSpace Repository

Theses and Dissertations 1. Thesis and Dissertation Collection, all items

1994-06

An experimental investigation of jet-induced ground effects and support strut interference on a STOVL configuration in hover

Dooley, William

Monterey, California. Naval Postgraduate School

http://hdl.handle.net/10945/30848

This publication is a work of the U.S. Government as defined in Title 17, United States Code, Section 101. Copyright protection is not available for this work in the United States.

Downloaded from NPS Archive: Calhoun

Calhoun is the Naval Postgraduate School's public access digital repository for research materials and institutional publications created by the NPS community. Calhoun is named for Professor of Mathematics Guy K. Calhoun, NPS's first appointed -- and published -- scholarly author.

Dudley Knox Library / Naval Postgraduate School
411 Dyer Road / 1 University Circle
Monterey, California USA 93943

http://www.nps.edu/library

NAVAL POSTGRADUATE SCHOOL
Monterey, California

THESIS

AN EXPERIMENTAL INVESTIGATION OF JET-INDUCED GROUND EFFECTS AND SUPPORT STRUT INTERFERENCE ON A STOVL CONFIGURATION IN HOVER

by

William Dooley

June 1994

Thesis Advisor:	S. K. Hebbar
Co-Advisor:	M. F. Platzer

Approved for public release: distribution is unlimited.

Thesis
D6496

DUDLEY KNOX LIBRARY
NAVAL POSTGRADUATE SCHOOL
MONTEREY CA 93943-5101

Unclassified
Security Classification of this page

REPORT DOCUMENTATION PAGE

1a Report Security Classification: Unclassified		1b Restrictive Markings
2a Security Classification Authority 2b Declassification/Downgrading Schedule		3 Distribution/Availability of Report Approved for public release; distribution is unlimited.
4 Performing Organization Report Number(s)		5 Monitoring Organization Report Number(s)
6a Name of Performing Organization Naval Postgraduate School	6b Office Symbol *(if applicable)* AA	7a Name of Monitoring Organization Naval Postgraduate School
6c Address *(city, state, and ZIP code)* Monterey CA 93943-5000		7b Address *(city, state, and ZIP code)* Monterey CA 93943-5000
8a Name of Funding/Sponsoring Organization NASA Ames Research Center	6b Office Symbol *(if applicable)* FFF	9 Procurement Instrument Identification Number
Address *(city, state, and ZIP code)* Moffet Field, CA 94035-1000		10 Source of Funding Numbers

Program Element No	Project No	Task No	Work Unit Accession No

11 Title *(include security classification)* AN EXPERIMENTAL INVESTIGATION OF JET-INDUCED GROUND EFFECTS AND SUPPORT STRUT INTERFERENCE ON A STOVL CONFIGURATION IN HOVER

12 Personal Author(s) Dooley, William

13a Type of Report	13b Time Covered	14 Date of Report *(year, month, day)*	15 Page Count
Master's Thesis	From To	June 1994	113

16 Supplementary Notation The views expressed in this thesis are those of the author and do not reflect the official policy or position of the Department of Defense or the U.S. Government.

17 Cosati Codes

Field	Group	Subgroup

18 Subject Terms *(continue on reverse if necessary and identify by block number)* STOVL Configuration in Hover, CALF Program, Jet-Induced Ground Effects, Ground-Plane Flow , Stagnation Streamline, Oil Flow Visualization, Support-Strut Interference

19 Abstract *(continue on reverse if necessary and identify by block number)*

A small-scale ground-effect test rig was designed and fabricated to study the ground-plane flow field generated by a STOVL aircraft in hover. The objective of the research was to support NASA Ames Research Center's planning for the upcoming large-scale powered model hover tests for the ARPA sponsored ASTOVL program. Specifically, small-scale oil-flow visualization studies were conducted to make a relative assessment of the aerodynamic interference of two proposed support-strut configurations on the ground-plane stagnation line. A simplified flat-plate model representative of a generic jet-powered STOVL aircraft with both the lift fan and the main engine simulated by air jets, with nozzle pressure ratios closely matching those of the large scale tests, was utilized. The flow visualization data clearly identified an aft shift in the stagnation line location for both strut configurations. Although the data indicated a slight reduction in the aft shift for the wider strut configuration, considering the experimental uncertainties involved it was concluded that either of the strut configurations caused only a minor aerodynamic interference.

20 Distribution/Availability of Abstract X unclassified/unlimited ___ same as report ___ DTIC users	21 Abstract Security Classification Unclassified	
22a Name of Responsible Individual Dr. S. K. Hebbar	22b Telephone *(include Area Code)* (408) 656-2997	22c Office Symbol AA/Hb

DD FORM 1473, 84 MAR 83 APR edition may be used until exhausted security classification of this page
All other editions are obsolete Unclassified

Approved for public release; distribution is unlimited.

An Experimental Investigation of Jet-Induced Ground Effects and Support Strut Interference on a STOVL Configuration in Hover

by

William Dooley
Lieutenant Commander, United States Navy
B.S., United States Naval Academy, 1978

Submitted in partial fulfillment
of the requirements for the degree of

MASTER OF SCIENCE IN AERONAUTICAL ENGINEERING

from the

NAVAL POSTGRADUATE SCHOOL
June 1994

Author: [redacted]
William Dooley

Approved by: [redacted]
S. K. Hebbar, Thesis Advisor

[redacted]
Max F. Platzer, Co-advisor

[redacted]
Daniel J. Collins, Chairman
Department of Aeronautics and Astronautics

ABSTRACT

A small-scale ground-effect test rig was designed and fabricated to study the ground-plane flow field generated by a STOVL aircraft in hover. The objective of the research was to support NASA Ames Research Center's planning for the upcoming large-scale powered model hover tests for the ARPA sponsored ASTOVL program. Specifically, small-scale oil-flow visualization studies were conducted to make a relative assessment of the aerodynamic interference of two proposed support-strut configurations on the ground-plane stagnation line. A simplified flat-plate model representative of a generic jet-powered STOVL aircraft with both the lift fan and the main engine simulated by air jets, with nozzle pressure ratios closely matching those of the large scale tests, was utilized. The flow visualization data clearly identified an aft shift in the stagnation line location for both strut configurations. Although the data indicated a slight reduction in the aft shift for the wider strut configuration, considering the experimental uncertainties involved it was concluded that either of the strut configurations caused only a minor aerodynamic interference.

Thesis
L6446
C.2

TABLE OF CONTENTS

I. INTRODUCTION 1
- A. BACKGROUND 1
- B. JET-INDUCED GROUND EFFECTS 3
- C. SCOPE OF THE THESIS 6

II. EXPERIMENTAL APPARATUS 8
- A. MODEL 8
  - 1. Scaling 8
  - 2. Nozzles 8
  - 3. Model Construction 9
- B. SUPPLY AIR 9
- C. GROUND PLANE 11
  - 1. Surface Platform 11
  - 2. Lift Mechanism 12
- D. STRUTS 12

III. EXPERIMENTAL PROCEDURE 17
- A. OIL DOT TECHNIQUE 17
  - 1. Composition Of Oil 17
  - 2. Application 19
- B. NOZZLE PRESSURE RATIO 20
  - 1. Thrust Ratio 20

DUDLEY KNOX LIBRARY
NAVAL POSTGRADUATE SCHOOL
MONTEREY CA 93943-5101

2. Setting The NPR 20

C. GROUND-PLANE HEIGHT 22

1. Specification 22

2. Setting The Height 22

D. PHOTOGRAPHY 23

E. MEASUREMENTS 24

IV. RESULTS AND DISCUSSION 27

A. EXPERIMENTAL ACCURACY 27

1. Measurements 27

2. Test Conditions 27

B. REPEATABILITY 28

1. Stagnation Point Measurements 28

2. Stagnation Line to Wingtip Measurements . . 28

3. Stagnation Line to Strut Measurements . . . 30

C. GROUND-PLANE FLOW FIELD VISUALIZATION 31

D. STAGNATION POINT LOCATION 32

1. NPR I (Thrust Ratio .67) 32

2. NPR II (Thrust Ratio .8) 34

3. NPR III (Thrust Ratio 1.1) 34

E. WINGLINE AND STAGNATION LINE INTERSECTION . . . 35

1. NPR I (Thrust Ratio .67) 36

2. NPR II (Thrust Ratio .8) 38

3. NPR III (Thrust Ratio 1.1) 38

F. STAGNATION LINE TO STRUT DISTANCE 41

1. NPR I (Thrust Ratio .67) 41

2. NPR II (Thrust Ratio .8) 43
3. NPR III (Thrust Ratio 1.1) 43

V. CONCLUSIONS AND RECOMMENDATIONS 46
A. CONCLUSIONS 46
1. Small Scale Model 46
2. NASA Ames LSPM OARF Implications 47
B. RECOMMENDATIONS 49
1. Experimental Apparatus 49
2. Experimental Procedure 49

APPENDIX A NOZZLE DESIGN 51

APPENDIX B GROUND-EFFECT TEST RIG DESIGN 52

APPENDIX C GANTRY CRANE WITH MODEL SUSPENSION SYSTEM . 53

APPENDIX D PROPOSED MODEL SUPPORT SYSTEM 54

APPENDIX E NOZZLE PRESSURE RATIO CALCULATIONS 55

APPENDIX F PHOTOGRAPHIC RECORD OF TEST RUNS 57

APPENDIX G EXPERIMENTAL RESULTS 89

APPENDIX H OPERATING INSTRUCTIONS 94

APPENDIX I ASYMMETRY OF GROUND-PLANE FLOW FIELD . . . 97
- A. DESCRIPTION 97
- B. CAUSE 99
    - 1. Lift Mechanism 99
    - 2. Ground Plane Border 100
    - 3. Nozzle Exit Plane 100
    - 4. Model Reference 100

LIST OF REFERENCES 102

INITIAL DISTRIBUTION LIST 103

ACKNOWLEDGEMENT

This thesis was funded by NASA Ames Research Center in support of the ongoing, ARPA sponsored, Common Affordable Lightweight Fighter program. The NASA support in the form of hardware and technical assistance is gratefully acknowledged. In particular, the assistance of Rich Margason and Larry Olsen is appreciated. Rich Margason was my principal contact at NASA and his technical expertise was invaluable to the successful completion of this study.

My deepest gratitude is extended to my thesis advisor, Professor S. K. Hebbar for his guidance, encouragement and untiring efforts to assist me in my work. I would also like to express my appreciation to my co-advisor, Professor M. F. Platzer, for his support. Professor T. Sarpkaya's timely assistance by way of loaning a Nikon camera deserves particular mention.

Special thanks are owed to Mr. Pat Hickey, Mr. Don Harvey and Mr. Ron Ramaker for their help in the design and fabrication of the test rig, high quality precision tooled nozzles and test models. The overall design, fabrication and day to day operation of the NPS Ground-Effect Test Rig would not have been possible without the insightful and skilled technical assistance of Mr. Rick Still and Mr. Thaddeus Best, which is gratefully acknowledged.

My greatest thanks go to my wife Linda and family for their continued support, selfless sacrifice and able assistance during this period.

I. INTRODUCTION

A. BACKGROUND

The Advanced Research Projects Agency (ARPA) has awarded contracts for the critical technology validation phase for the Advanced Short-Take-Off and Vertical Landing (ASTOVL) aircraft. The replacement of the aging fleet of AV-8B Harriers is one of the prime objectives. In addition to the well defined Marine Corps requirement the ASTOVL aircraft may in fact be able to match the performance characteristics and replace conventional carrier based aircraft of the U.S. Navy. It is also hoped that the ASTOVL, with minimal changes, will be a suitable replacement for the USAF conventional take-off and landing (CTOL) F-16 Falcon [Ref. 1].

While the ultimate role of the ASTOVL is still many years and budget battles away the actual development of design proposals is being conducted by Lockheed Advanced Development Company (LADC), McDonnell Douglas (MD) and Boeing. Contracts were initially awarded in March of 1993 to LADC and MD for the technology validation phase consisting of a series of rig, model and simulator tests. Since that time Boeing has submitted its own proposal which will be included in the design competition. Large scale powered rigs will test the proposed powered lift systems. Large scale powered models (LSPMs) will

be tested at NASA Ames 80′ x 120′ wind tunnel, testing the models in the hover mode and the transition to low speed forward flight. The airframes will also be tested in the NASA Ames Outdoor Aerodynamic Research Facility (OARF) by supporting the models on struts and running the engines. This will allow for a careful analysis of the complex airflows around the aircraft including the propulsive lift parameters, jet-induced ground effect and hot gas ingestion characteristics. Flight simulation will take place in the NASA Ames vertical motion simulator. Based on the competing performance evaluations ARPA will select a design for prototype production in 1996 with a projected first flight as early as 1998.

The design proposals for the MD and LADC aircraft have many similarities. Both designs will incorporate a fuselage mounted lift fan placed aft of the cockpit to support the nose of the aircraft during VTOL flight. This fan will be powered by a single after burning turbofan engine producing 40,000 lbs of thrust. The major difference in the two design proposals is the method of powering the forward lift fan. The LADC proposal will utilize a Pratt & Whitney consortium shaft-driven lift fan (SDLF) concept. The forward lift fan will be mechanically linked through a drive shaft and gearbox to the main engine. During VTOL flight a thrust-vectoring nozzle will

divert exhaust flow downward to support the tail.

The MD design has a gas-driven lift fan (GDLF) which will utilize a General Electric propulsion system. This system will divert air from the single turbofan engine directly to the forward lift fan with no direct mechanical connection between the components. Figures 1 and 2 show the respective LADC and MD ASTOVL designs [Ref. 2].

In order to conduct the large scale OARF tests the optimum placement of the supporting struts is of critical importance. Small-scale flow visualization tests of the jet-induced ground effects and the effect of support struts on fountain formation caused by the impingement and subsequent interaction of vertical jets on the ground plane will assist in the qualitative understanding of the flow patterns induced by the strut interference. The flow visualization data can be used to help identify the optimum location for the support struts to minimize the interference with the flow field.

B. JET-INDUCED GROUND EFFECTS

The ground effect associated with a conventional aircraft is a well understood phenomenon; especially to pilots who rely on the increased lift to cushion their touchdowns during flared landings. With STOVL aircraft the overall jet-induced ground effect can produce a suckdown or loss of lift as well

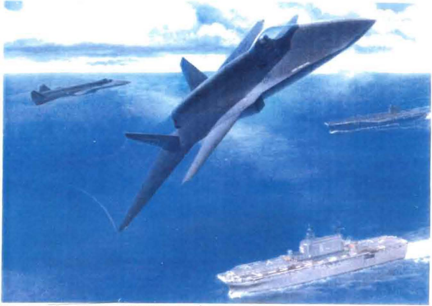

Figure 2. MD ASTOVL Design

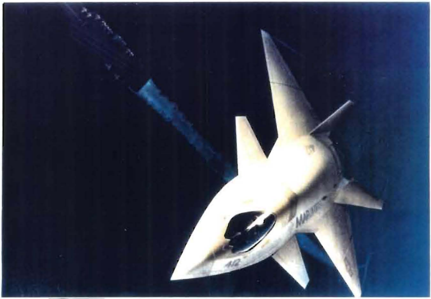

Figure 1. LADC ASTOVL Design

as a positive lift depending on the height above the ground. The flow field elements of a dual lift jet aircraft in ground effect are shown in Figure 3.

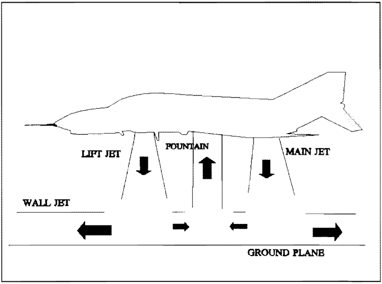

Figure 3. Flow Field for STOVL Aircraft Hovering in Ground Effect

The support force for the aircraft is produced by the two jets pointed downward. As the jets impinge on the ground a wall-jet effect is produced parallel to the ground plane radiating outward. The primary jets and the wall-jet entrain air beneath the surface of the aircraft reducing the pressure and the net lift. With two or more lift jets present a fountain upwash flow is formed between the impinging jets. This fountain flow will act on the underside of the aircraft increasing the pressure and the net lift. The overall net lift can vary greatly depending on aircraft configuration with the suckdown, negative lift, dominating at lower heights above the ground plane [Ref. 3].

The understanding of the flow field and the fountain formation is a key factor when trying to account for all forces and moments imposed on the aircraft in ground effect. During the LSPM OARF tests the interference caused by the support struts and their effect on the stagnation line location and subsequent fountain flow must be determined in order to accurately assess the aircraft's lift system performance both in and out of ground effect.

C. SCOPE OF THE THESIS

The aim of this thesis was to support NASA Ames Research Center's planning for LSPM hover tests for the ARPA sponsored Common Affordable Lightweight Fighter (CALF) program. Specifically, it was aimed at conducting small scale flow visualization studies in the Naval Postgraduate School (NPS) ground-effect test rig on a simplified flat-plate configuration representative of a generic jet-powered STOVL aircraft in hover. The jet-induced ground effects and the support-strut interference were determined by oil flow technique on the ground-plane.

The general procedure followed here consists of comparing the ground-plane flow pattern and the stagnation line location produced by the model with and without the support struts. The two strut configurations chosen for this investigation were based on the proposed strut locations for the NASA Ames OARF tests. Likewise, the seven ground-plane heights and the three nozzle pressure ratios selected covered the anticipated range of the LSPM testing.

It is hoped that the flow visualization data will provide crucial input for the design of the upcoming LSPM testing at NASA Ames Research Center.

II. EXPERIMENTAL APPARATUS

A. MODEL

1. Scaling

The major consideration in determining the appropriate scale factor was the relative size of the model's jet nozzles compared to the LSPM [Ref. 4]. The exit area of the LSPM lift fan was used to determine an equivalent diameter. This value was compared to the diameter of the forward nozzle of the mode which was one inch. The rear nozzle had a diameter of 1.1 inch. The length and wing span of the model were selected to be consistent with the NASA Ames generic configuration.

2. Nozzles

The nozzles were designed to provide the required exit diameter for the scale factor used. The supply air was fed from two inch piping. The nozzles were fabricated to provide a flush fit with the supply pipe and a simple converging passage from a two-inch diameter to a one-inch diameter. Access for a pitot tube was provided to ensure accurate pressure settings. Schedule 80 steel piping used was rated for an air pressure of 300 psi. Appendix A displays the nozzle design.

3. Model Construction

LADC and MD have both developed similar airframes for their ASTOVL programs. In order to avoid proprietary considerations a generic design was used for this thesis study. Characteristics of both the LADC and the MD airframes were combined so that the test model could be used to represent either design. However, since the scale factor was determined by the exit area of the lift fan and these areas are different for the LADC and MD designs different scale factors are required. This necessitates the use of different models to represent the LADC or the MD design. An alternative approach would be to use the same model but different nozzles.

A 1/2-inch-thick plexiglass was utilized for the model construction with a length of 22.25" and a wing span of 18.63". Although a beveled edge is considered to produce a more accurate representation of the resulting lift loss [Ref. 4], it was not critical for the qualitative assessment of the effects on the ground-plane. A flat plate design with square edges was therefore used for ease of construction. The model is shown in Figure 4.

B. SUPPLY AIR

The high pressure air for the ground-effect test rig was supplied from the existing facilities at the Naval Postgraduate School Gas Dynamic Laboratory. The facility

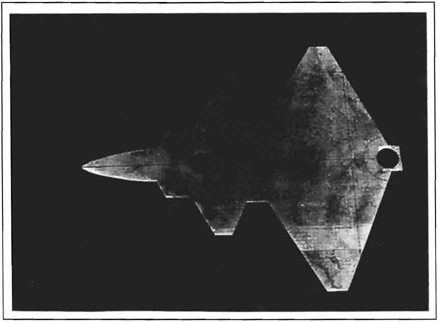

Figure 4. Generic Test Model

provides 8000 cubic feet of air at 300 psia when both of its compressors are operating. During the test period only one compressor was operational providing 150 psia.

It was necessary to tap into an existing four-inch supply line. NASA Ames provided the necessary hardware and assisted in the installation. A 4" x 3" x 4" tee was inserted into the existing line to provide a new three-inch supply line, which was fitted with a three-inch gate valve to act as air supply shut off control. A 2" x 3" x 2" tee was installed downstream of the gate valve to provide the required two-inch supply lines to the nozzles. Two regulator valves were provided for independent pressure control to the nozzles. Appendix B shows the design for the ground-effect test rig displayed in Figure 5.

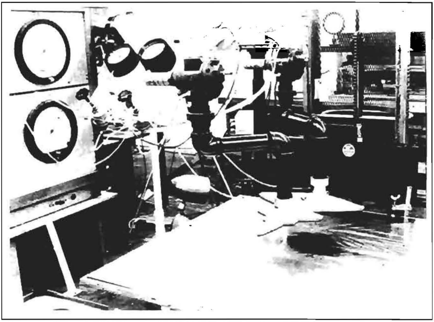

Figure 5. NPS Ground Effect Test Rig

C. GROUND PLANE

1. Surface Platform

A 46-inch square wooden frame with an aluminum tray cemented on top served as the test surface. The size of the test model dictated the relative size of the test platform. Testing conducted at NASA Ames concluded that the ground board size need only be as large as the model since the suction is generated mainly by the ground jet beneath the surface of the model [Ref. 3]. Initially the wooden frame contained a one-inch border with the aluminum tray recessed below the top of the border to prevent the oil from running off the platform. This border was later removed when it was determined that there was no need to contain the oil flow.

2. Lift Mechanism

In order to easily change the height of the ground plane the test surface was placed on a hydraulic lift. While this facilitated varying the height of the ground plane it also complicated the problem of maintaining a level plane with the nozzles. The lift was designed for heavy loads; not for precise experimental measurements. Wedges were placed under the test frame to ensure the ground plane was parallel to the exit plane of the nozzles.

D. STRUTS

NASA Ames initially proposed a crane/cable model support system for the OARF powered-model tests planned for 1995. This type of system was attractive due to the relative ease of changing heights and non-interference with the ground and fountain-flow formation. An estimate of 18 months to design, build and checkout such a system was considered too expensive to pursue. The alternative approach was to use existing model struts designed for the 80′ x 120′ wind tunnel. These struts would support an overhead frame that the model would be suspended from. The crane/cable suspension system and proposed support structure are depicted in Appendixes C and D.

The optimum strut placement of necessity would be a compromise between structural support considerations and the desired minimum effect on the ground stagnation line and ultimate fountain formation. Two main struts and one nose strut would be necessary to provide the required support. The small scale tests conducted at the NPS Ground-Effect Test Rig were specifically tailored to help determine this optimum strut placement.

The struts used in this study were simplified to a constant cylindrical shape. Scaling was accomplished by applying the established scale factor (determined from the nozzle considerations) to the circumference of the actual struts. Two strut configurations were studied based on the proposed strut locations for the NASA Ames OARF tests.

For the first configuration wooden dowels were used with a main strut diameter of 1.44" and a nose strut diameter of .375". The actual strut placement at the OARF, which is limited by hardware constraints, results in a 50' distance between the main struts and a 50' distance from the axis of the main struts to the nose strut. The scaled placement of the struts is depicted in Figure 6.

For the second configuration PVC tubing was used for the main struts with a diameter of 1.92". The same wooden dowel from the first configuration, with a diameter of 1.44", was used for the nose strut. The OARF strut placement for this configuration maintains the same 50' distance from the axis of the main struts to the nose strut but increases the distance between the main struts to 80'. Additionally, the LSPM is moved 6' aft relative to the main strut axis. The scaled placement of the struts for this configuration is depicted in Figure 7.

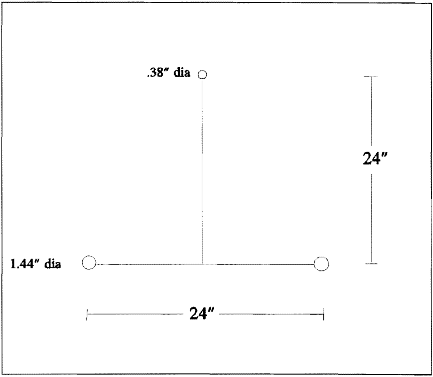

Figure 6. Strut Position Configuration 1.

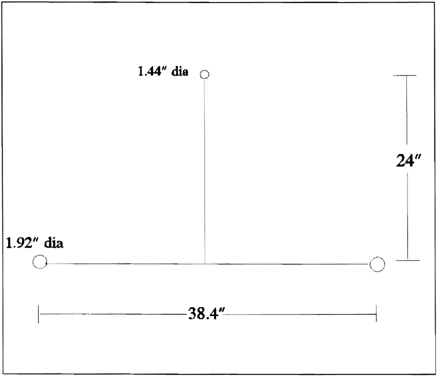

Figure 7. Strut Position Configuration 2.

III. EXPERIMENTAL PROCEDURE

A. OIL DOT TECHNIQUE

1. Composition Of Oil

The ground-plane flow visualization was accomplished by placing a mixture of oil and fluorescent paint pigments on the ground plane and allowing the mixture to react to the exhaust stream of the model's two jets. The ground flow streamline patterns formed clearly delineated where the jet flows impinged on the ground plane [Ref. 6]. The use of paint pigments to produce different colors provided an excellent contrast when comparing the surface streamlines. This contrast was further enhanced by the use of ultra violet lighting which produced a dramatic effect due to the fluorescent nature of the paint pigments.

For this study standard grade motor oil (Pennzoil 10W40) was selected. Additionally, STP Oil Treatment was added to the Pennzoil to produce a thicker, more viscous solution. The desired consistency was achieved through a trial and error process with the preferred mixture having a ratio of 5:1 by volume of motor oil to STP. This produced a solution that could be easily applied to the ground plane by small squeeze bottles. The eye-dropper sized applicator produced a uniform drop of oil that would not spread excessively prior to the jets being activated.

Fluorescent paint pigments were added to the oil to produce a colored mixture. Four pigment samples (rocket red, aurora pink, blaze orange and saturn yellow) were provided by the Day-Glo Color Corporation of Cleveland, Ohio. The exact amount of pigment sample required was a subjective decision based on the brightness of the color desired. For the purpose of this experiment two ounces (by volume) of powdered paint pigment was mixed with eight ounces of oil. Mixing was accomplished by the use of a magnetic stirrer. The materials used, magnetic stirrer and oil mixture applicator are displayed in Figure 8.

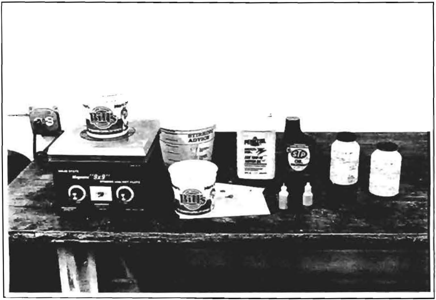

Figure 8. Oil Mixture Materials

2. Application

The oil dot technique was chosen over a brush-type application to study the local surface streamline pattern [Ref. 7]. In order to produce consistent spacing of the oil dots on the ground plane a 3/4"-thick plywood template was constructed with 1/4"-diameter holes drilled 2" apart. The template matrix of 17 x 17 holes facilitated the rapid and evenly spaced distribution of oil dots as shown in Figure 9.

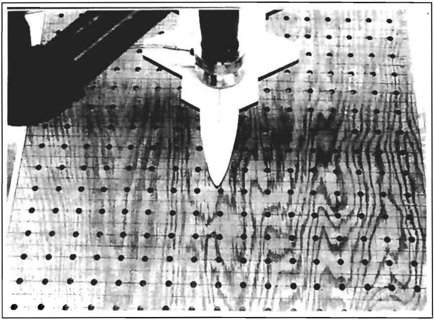

Figure 9. Template For Oil Dot Application

Additional dots of oil were placed in areas of critical interest; such as in the proximity of the stagnation line and around the strut locations.

B. NOZZLE PRESSURE RATIO

1. Thrust Ratio

The NPRs were chosen to produce the desired thrust ratio between the aft (main) nozzle and the forward (lift) nozzle. The thrust ratios were chosen to match the range of thrust ratios that will be used for the NASA Ames OARF tests. Three thrust ratios, .67, .8 and 1.1, were selected to cover this range and the associated nozzle pressure ratios are referred to as NPR I, NPR II and NPR III. The method of determining the NPR of the nozzles is shown in Appendix E and is in accordance with established NASA Ames Research Center procedures [Ref. 8].

2. Setting The NPR

The forward and aft nozzles can be controlled independently utilizing separate pressure regulator valves. The resulting pressure can be read from the connected pressure gages as shown in Figure 10. These gages were difficult to read due to the large scale and did not account for the losses associated with the final two 90° bends in the supply air piping. In order to obtain a more accurate reading of the actual pressure at the nozzle exit a dual set of pressure gages with finer resolution were utilized to record the pitot probe readings at the nozzle convergence passage as shown in Figure 11.

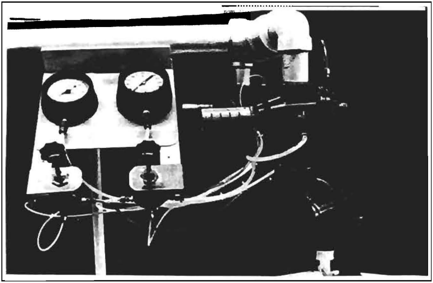

Figure 10. Independent Nozzle Regulator Control Valves

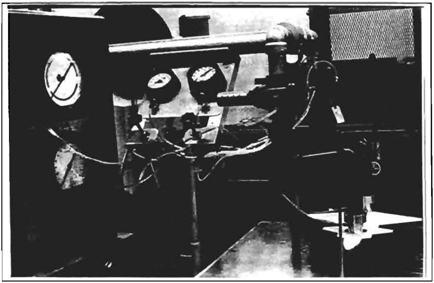

Figure 11. Nozzle Pressure Gages

C. GROUND-PLANE HEIGHT

1. Specification

A preferred method of referencing the height of a STOVL aircraft above the ground plane is to use the ratio of the height of the aircraft to the equivalent diameter of the combined exit area of all nozzles (h/D_e). The OARF tests will be conducted at h/D_e values of 1-15. Values of h/D_e= 1,2,4,6,8,10 and 15 were chosen to match the OARF range of study. The lowest value of h/D_e corresponds to the lowest height that the LADC model will be tested at with its four-foot gear height. The high value of h/D_e is at the edge of the ground effect height.

2. Setting The Height

Prior to making any height settings the lift mechanism was raised in order to trace the outline of the model on the ground plane. This provided an ideal reference frame for all measurements. Once the model had been traced the lift was lowered in order to place the oil dots on the ground plane using the plywood template as a guide. The ground plane was then raised to just below the model surface to ensure the alignment with the traced outline was still valid. Minor adjustments to the positioning of the ground plane could be made if required. At this time the ground plane was lowered by the hydraulic lift to the appropriate distance. Measurements were made from both wingtips, both canards and from the nose of the model to the ground plane to ensure that the model was in fact level with the ground plane. Small wooden wedges were positioned between the lift tray and the underside of the ground plane to correct any deviations to the level plane of the nozzle exit area.

At the conclusion of the nozzle run (lasting approximately five minutes) the distances from the wings, canards and nose were again measured to ensure that the ground plane had not shifted during the experiment.

D. PHOTOGRAPHY

This study was conducted in order to determine the effect the strut placement would have on the formation of the ground stagnation line. In order to have visual documentation of the results photographs were taken at the completion of all test runs and are displayed in Appendix F. A Nikon F3 camera with a 35-105 mm lens was used. The ground plane was lowered to a minimum lift height for all photographs producing a focal length of five feet. Two sets of photos were taken; one using normal overhead lighting and the other utilizing two 115V 2Amp portable ultraviolet lights.

The camera was mounted on a tripod placed at the front of the ground-plane test platform. This resulted in an angled overhead view providing excellent perspective to the stagnation line formation. The camera required manual focusing but was equipped with an auto-exposure feature that adjusted the shutter speed to the selected aperture opening of f5.8. Black and white ASA 400 film was used.

Color photographs of selected runs were obtained using a Minolta 5000i Maxima camera with a 50/1.4 mm lens. This camera featured both auto-focus and auto-exposure functions and was tripod mounted resulting in a focal length of six feet. Color ASA 400 film was used.

E. MEASUREMENTS

The primary method of comparing the test results was through the photographic record of all test runs. Measurements were taken to quantify the visual results, as shown in Figure 12.

A stagnation point forms on the ground plane where the wall-jet velocities of the forward and rear nozzles cancel each other. The dividing streamline that passes through the stagnation point marking the wall-jet boundaries on either side is called the stagnation streamline, or stagnation line for short. The nose of the model was used as a reference point and the distance to the stagnation point was measured for all test runs.

The radius of curvature of the stagnation line varies along the line and changes with the different test conditions. In order to quantify this result two additional measurements

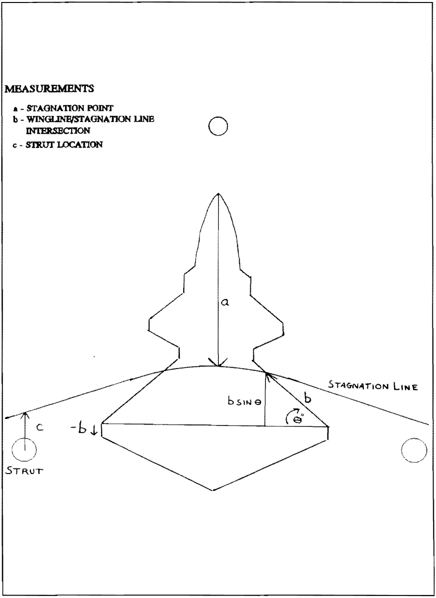

Figure 12. Measurements of Ground Stagnation Line

were taken. (i)The distance from the forward part of the wing tip to the intersection of the stagnation line with the wing line was measured. The perpendicular distance (b$\sin\theta$ in Fig.12) from the wingtip line to the intersection of the stagnation line with the wing line was used for comparative analysis. Negative values for the measurements indicate that the stagnation line is aft of the forward part of the wingtip. The distance for the negative values is measured from the forward part of the wingtip aft along the wingline to the intersection of the stagnation line. (ii)The distance from the center of the strut position to the stagnation line was also measured.

Once the final measurements were taken the ground plane was cleaned with a paint thinner solution. The experimental procedure was then repeated for the next h/D_e setting. Tables 1-9, Appendix G, list all the measurements made on the ground-plane. A detailed experimental procedure is outlined in Appendix H.

IV. RESULTS AND DISCUSSION

A. EXPERIMENTAL ACCURACY

1. Measurements

The ground-plane measurements were made with a tape measure having 1/16" graduations. The exact location of the stagnation line was a subjective decision due to the 1/8" width of the line. The measurements taken from the traced outline of the model on the ground plane induced minor inaccuracies. Additionally, the stagnation point was not well defined at the ground-plane height of 22.25" ($h/D_e = 15$). The measurement error was estimated to be ± 1/16".

2. Test Conditions

In order to compare the test results between the various strut configurations it was necessary to reproduce the test conditions. The setting of the NPR's, adjustment of the ground-plane height and orientation of the jet exit-plane were critical factors. While every effort was made to reproduce these parameters small variations were unavoidable contributing to the experimental uncertainty.

B. REPEATABILITY

To assess the repeatability of the test data two independent experimental runs, utilizing the same test conditions, were compared. The test condition corresponding to NPR I, with no struts, was selected for the comparison. The results are discussed below:

1. Stagnation Point Measurements

The results of stagnation point measurements for two runs are displayed in Figure 13. The distances from the nose of the model to the stagnation point were, on the average, 1/8" different for the two runs. The maximum difference was 1/4" at a ground-plane height of 3" ($h/D_e = 2$). The difference at each of the heights 9", 12" and 15" ($h/D_e = 6,8,10$) was only 1/16".

2. Stagnation Line to Wingtip Measurements

Figure 14 displays these results for two identical runs. The existence of an asymmetric flow pattern, which is discussed in Appendix I, required the right and left measurements to be compared separately. The overall average difference in the measurements between the two runs was .201". The average difference in the computed perpendicular distance to the wingtip line ($b\sin\theta$, Figure 12) was .123". The maximum measured difference was 5/16" at a ground-plane height of 6" ($h/D_e = 4$) for the left wing.

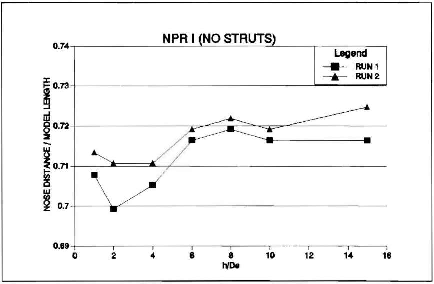

Figure 13. Repeatability of Stagnation Point Measurements

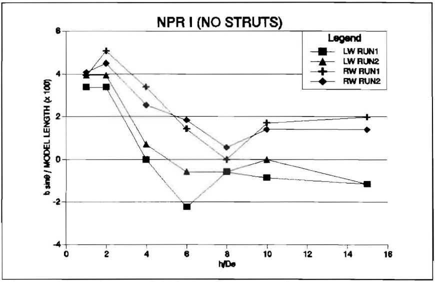

Figure 14. Repeatability of Stagnation Line to Wingtip Measurements

3. Stagnation Line to Strut Measurements

The results of these measurements for two runs are displayed in Figure 15. While the comparative test runs did not include struts, the distance from the center of the proposed strut location for configuration 1 was still measured. The maximum difference in the measurement between the two test runs was 7/16" at a ground-plane height of 9" (h/D_e = 6). The overall average difference was .214".

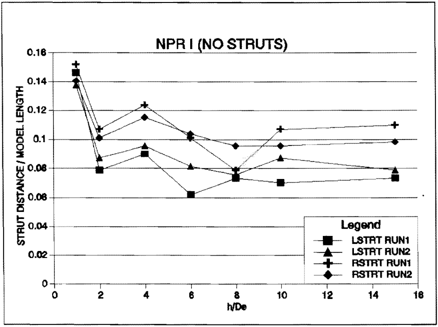

Figure 15. Repeatability of Stagnation Line to Strut Measurements

C. GROUND-PLANE FLOW FIELD VISUALIZATION

Predictions of the location of the ground-plane stagnation line utilizing a computer program based on the "Momentum Flux Density Method" have proven to be quite reasonable [Ref. 9]. However, extension of 2-D potential methods to 3-D flow fields to predict ground effects and strut interference is quite a challenging task. By studying the photographic records of the test results (see Appendix F) the effects of ground-plane height, NPR and strut location on the stagnation line can be visibly seen. Of particular note is the marked change in the geometric pattern that develops from increasing the h/D_e value. This effect can be clearly seen in an examination of NPR II over the range of heights studied. The stagnation line transitions from an initial convex orientation (with respect to the model nose) at the lower heights to a concave orientation at the upper heights.

A similar geometric shift in the ground stagnation line was produced by the addition of struts. This effect is clearly documented for NPR II at a ground-plane height of 3" ($h/D_e = 2$). An initial convex orientation was shifted to a concave pattern when strut configuration 1 was included .

In many instances the shift in the ground-plane flow pattern was very subtle. The effects of the ground-plane height, NPR and strut configuration on the ground-plane stagnation line were examined by quantifying the location of the stagnation line. These effects are discussed in the following sections.

D. STAGNATION POINT LOCATION

The placement of struts on the ground plane produced a definite aft shift of the stagnation point for all NPR's and both strut configurations. In most cases the shift was less than the maximum scatter of .25" observed during the repeatability analysis. As would be expected the aft shift became less pronounced as the NPR's were increased due to the increased thrust from the rear nozzle. A detailed analysis of the results for each NPR is given below:

1. NPR I (Thrust Ratio .67)

Figure 16 displays the results for NPR I, with and without struts. The average aft shift when compared to run 1 for strut configuration 1 was .205" while the average aft shift for configuration 2 was .196". The difference in the shift between the two configurations was less than 1/16". If these aft shifts were compared to run 2, which was taken for the repeatability analysis, the shifts would be .080" and .071" for configurations 1 and 2 respectively. These shifts, while noticeable and consistent, are within the experimental uncertainty.

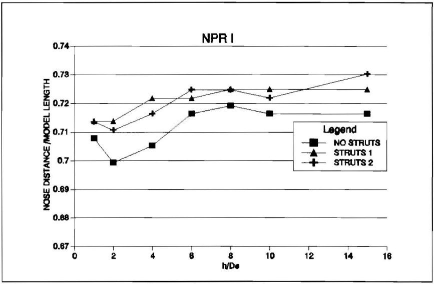

Figure 16. Stagnation Point Location for NPR I

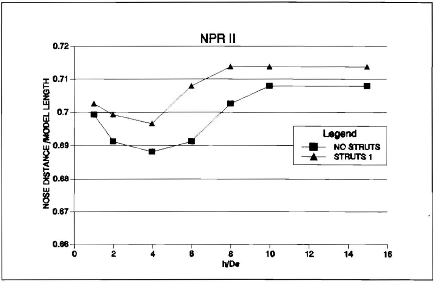

Figure 17. Stagnation Point Location for NPR II

2. NPR II (Thrust Ratio .8)

The results from the comparison between no struts and configuration 1 were very similar to the NPR I case and are displayed in Figure 17. Strut configuration 2 was not tested for this NPR. A definite, consistent aft shift was detected over the entire range of ground-plane heights but the magnitude of the shift was within the experimental uncertainty. An average shift of .188" was observed with the largest shift of .375" occuring at a height of 9" ($h/D_e = 6$).

3. NPR III (Thrust Ratio 1.1)

NPR III produced the smallest aft shift in the stagnation point location and the results are displayed in Figure 18. Strut configuration 1 produced an average shift of .107" while configuration 2 produced a shift of .063". The aft shift of the stagnation line was very small for both strut configurations with the largest shift of .25" occuring at 1.5" and 22.25" ($h/D_e = 1,15$). The shifts for the intermediate heights were much smaller. While the aft shift for strut configuration 2 was less than that for configuration 1 the magnitude of the shift for both configurations was within the experimental scatter, precluding any conclusions from being drawn.

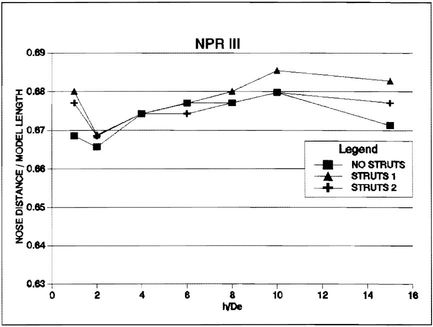

Figure 18. Stagnation Point Location for NPR III

E. WINGLINE AND STAGNATION LINE INTERSECTION

The intersection of the stagnation line with the wingline displays the same aft-shift trend as the stagnation point when the struts are added to the ground plane. Again, due to the asymmetry, the left and right intersections were analyzed separately. The computed perpendicular distance, b $\sin\theta$, behaves in a linear fashion both fore and aft of the wingtip line. For this reason it was used for comparison vice the actual measured distance along the wingline to the stagnation line intersection. Due to the 30° sweep of the model wingline the value b $\sin\theta$ equates to b/2 making for a simple calculation. As explained in Chapter III, Section E, when the stagnation line forms aft of the forward part of the wingtip ($\theta = -90^\circ$) b $\sin\theta$ equates to -b. Again, as expected, the aft shift became less pronounced as the NPR was increased due to the increased value of the rear nozzle thrust. A detailed analysis for each NPR is given below:

1. NPR I (Thrust Ratio .67)

The aft shift of the perpendicular distance of the stagnation line intersection to wingtip distance (b $\sin\theta$) is displayed in Figures 19 and 20 for the left and right wings, respectively. The shift was more pronounced for the left wing than for the right wing for both strut configurations. Also, the left intersection behaved as expected with the shift being more pronounced for strut configuration 1, which was closer to the model, than configuration 2. The results for the right wing indicated that the shift was slightly more pronounced for strut configuration 2. The difference between the shifts for the two configurations was only an average of .058" for the right wing. This was less than the experimental scatter. The effects of the asymetric flow and the scatter in the data are suspected to be the source of apparent inconsistent results between the left and right wing.

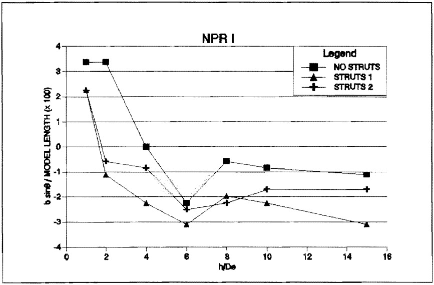

Figure 19. Stagnation line Intersection to Wingtip Distance for NPR I (Left Wing)

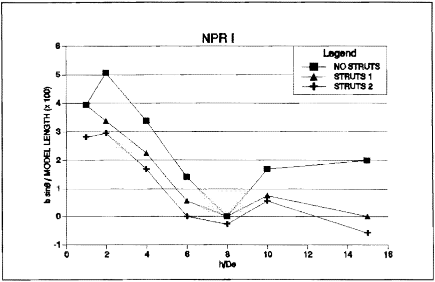

Figure 20. Stagnation Line Intersection to Wingtip Distance for NPR I (Right Wing)

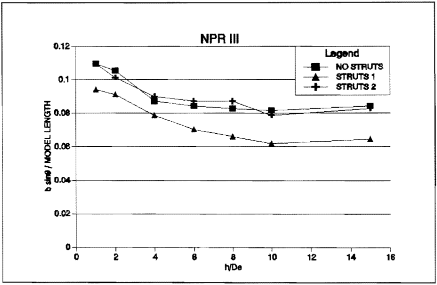

Figure 23. Stagnation Line Intersection to Wingtip Distance NPR III (Left Wing)

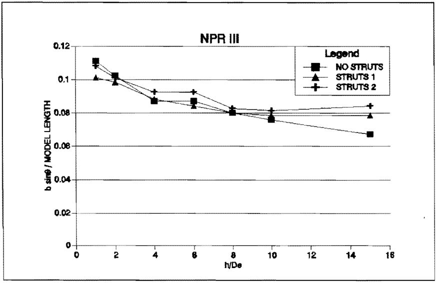

Figure 24. Stagnation Line Intersection to Wingtip Distance NPR III (Right Wing)

F. STAGNATION LINE TO STRUT DISTANCE

This distance was measured for the no strut configuration and strut configuration 1 to provide an additional reference point to compare the effect of the strut placement on the curvature of the stagnation line. Since the strut placement was different for strut configuration 2 the comparative value of such a measurement was not considered relevant and was, therefore, not taken. It was noted before (see Sections D & E) that the average aft shift for the nose and wingtip measurements decreased as the NPR was increased. This trend did not hold true for the stagnation line to strut measurements. Despite the fact that the rear nozzle produced more thrust as the NPR was increased from I to III the effect of the strut was strong enough to overcome the expected forward movement of the stagnation line caused by the increased thrust. A detailed analysis of the stagnation line to strut measurements is presented below:

1. NPR I (Thrust Ratio .67)

The aft shift was more pronounced for the lower ground-plane heights and is displayed in Figures 25 and 26 for the left and right struts, respectively. The average shift for both struts was .521" over the first three ground-plane

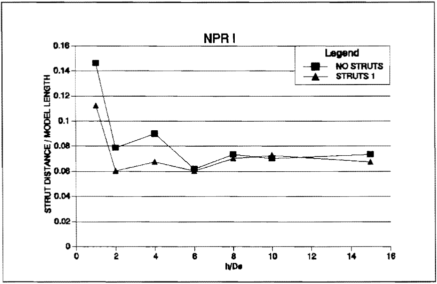

Figure 25. Stagnation Line to Strut Distance for NPR I (Left Strut)

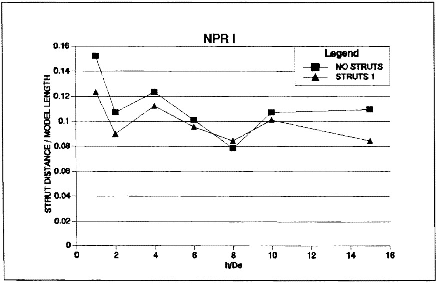

Figure 26. Stagnation Line to Strut Distance for NPR I (Right Strut)

heights of 1.5", 3.0" and 6.0" ($h/D_e = 1,2,4$). Above this height the shift was inside the experimental uncertainty, excepting the measurement for the 22.25" height ($h/D_e = 15$) for the right strut.

2. NPR II (Thrust Ratio .8)

The aft shift was fairly constant over the entire range of ground-plane heights and is displayed in Figures 27 and 28 for the left and right struts, respectively. The average shift was .464" for the left strut and .438" for the right strut with a maximum shift of .938" for the right strut at a ground-plane height of 9" ($h/D_e = 6$).

3. NPR III (Thrust Ratio 1.1)

The aft shift is displayed in Figures 29 and 30 for the left and right struts, respectively. The aft shift for the left strut remained fairly constant over the entire range of ground-plane heights with an average value of .732". The shift for the right strut was not as pronounced and tapered off to values below the experimental uncertainty for ground-plane heights above 9" ($h/D_e = 6$).

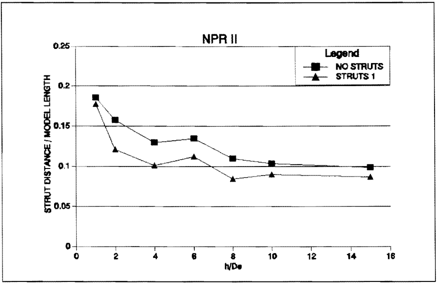

Figure 27. Stagnation Line to Strut Distance for NPR II (Left Strut)

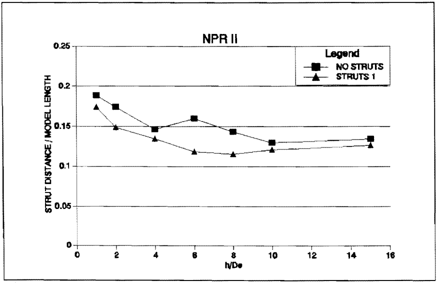

Figure 28. Stagnation Line to Strut Distance for NPR II (Right Strut)

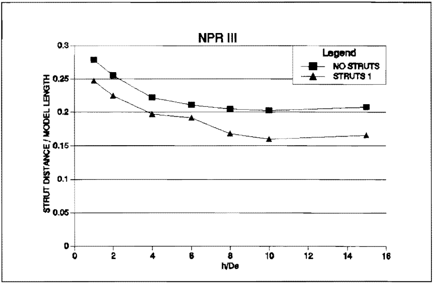

Figure 29. Stagnation Line to Strut Distance for NPR III (Left Strut)

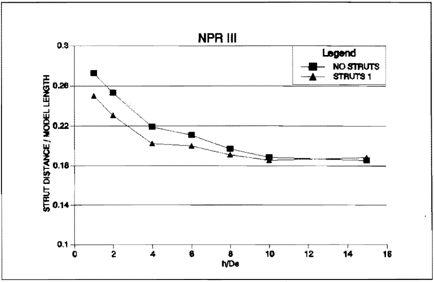

Figure 30. Stagnation Line to Strut Distance for NPR III (Right Strut)

V. CONCLUSIONS AND RECOMMENDATIONS

A. CONCLUSIONS

At the request of NASA Ames Research Center, an experimental investigation of the ground-plane flow field generated by a STOVL aircraft in hover was conducted to evaluate the support-strut interference on the formation of the ground-plane stagnation line. An oil-flow visualization study was conducted to make a relative assessment of the aerodynamic interference of two proposed support-strut configurations.

1. Small-Scale Model

The location of the stagnation line was found to shift when dowels simulating support struts were placed in the vicinity of the model. The ground-plane streamlines produced by the the two jets were forced to alter their path due to the presence of the struts. The resulting ground stagnation streamline location reflected the combined shift of the contributing streamlines of the two jets as they opposed each other. Table 10 summarizes the experimental data showing the average aft shift of the stagnation line, by strut configuration, for each of the three NPRs. The aft shift quoted is the average value taken over all the ground-plane heights tested.

TABLE 10: AVERAGE AFT SHIFT OF STAGNATION LINE DUE TO STRUTS

DISTANCE MEASURED	SCATTER BAND	STRUT CONFIG	NPR I	NPR II	NPR III
STAG. POINT	.125	STRT 1	.205	.188	.107
		STRT 2	.196		.063
WINGLINE $(b\sin\theta)$ LW/RW	.123	STRT 1	.429/.205	.303/.268	.344/.103
		STRT 2	.295/.263		.058/.129
STRUT LW/RW	.214	STRT 1	.268/.373	.464/.438	.732/.268

(ALL MEASUREMENTS IN INCHES)

The shift in the stagnation point was slightly more pronounced for strut configuration 1. However, the difference in the shifts between the two configurations was less than the experimental uncertainty in most cases making a definitive conclusion difficult. The trends in the stagnation line did suggest that the closer proximity of strut configuration 1 did in fact have a greater influence on the stagnation line shift.

2. NASA Ames LSPM OARF Implications

The experimental results scaled for the LSPM are displayed in Table 11. Again the difference between the shift of the stagnation line is so small that one strut configuration cannot be assumed to be less disruptive than the other.

TABLE 11: AVERAGE AFT SHIFT OF STAGNATION LINE SCALED TO LSPM

DISTANCE MEASURED	SCATTER BAND	STRUT CONFIG	NPR I	NPR II	NPR III
STAG. POINT	3.00	STRT 1	5.13	4.70	2.68
		STRT 2	4.90		1.58
WINGLINE (bsinθ) AVE	2.95	STRT 1	7.93	7.14	5.59
		STRT 2	6.98		2.34
STRUT AVE	5.14	STRT 1	8.01	11.28	12.50

(ALL SCALED VALUES IN INCHES)

The decision to use strut configuration 2 has been made by NASA Ames. This decision was based on structural support considerations and the increased capability to handle models of different size. The results of this study confirmed their belief that nothing would be lost by choosing the wider strut configuration and there would be no unforeseen strut interference with the ground-plane stagnation line. In fact, the more pronounced, undesirable stagnation line shift around the wingtip due to the closer proximity of strut configuration 1 to the model, would be reduced by utilizing strut configuration 2. Additionally, the forces experienced by the support struts will be less, which is desirable because of the multitude of control cables and electrical wiring in this area.

B. RECOMMENDATIONS

1. Experimental Apparatus

The existing facilities can be improved to increase the level of precision, accuracy and repeatability of test conditions for the NPS Ground Effect Test Rig. The following recommendations are based on the procedures developed for this investigation:

a. Acquire a dedicated lift mechanism with a self-leveling feature that can be precisely set to the desired ground-plane height.

b. Attempt to eliminate the undesired swirl which is imparted to the jet flow by the supply piping. This will minimize the asymmetry in the jet stream.

c. Purchase a 35-105 mm zoom lens for the Minolta 5000i Maxima camera to capture the entire ground plane in the field of view.

2. Experimental Procedure

Ideally a large sample of test runs should be conducted at different NPRs so that a meaningful statistical analysis could be performed on the repeatability of the test conditions. Due to time constraints only one NPR was checked for repeatability with only two sets of data for comparison.

Additional testing to further investigate the interaction between the stagnation line location and the strut placement on the formation of the fountain flow and the resulting forces experienced by the model is called for. Visualization of fountain formation using water-spray injection technique is strongly recommended. To fully understand the forces involved it would be desirable to have pressure measurements on both the underside of the model and the ground plane.

The turbulent flow field generated around the wingtips of the model is another area of concern that calls for a full understanding of support strut interference effects. A LDV study is currently being conducted as a follow-on thesis project to investigate this matter.

APPENDIX A

NOZZLE DESIGN

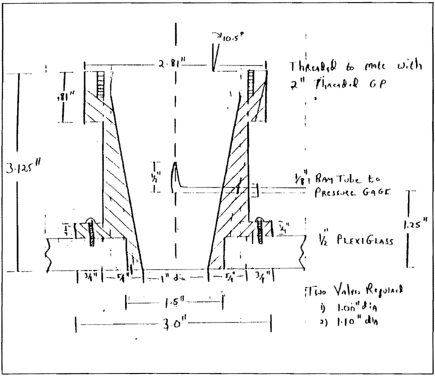

Figure 31. 1" Nozzle Design

APPENDIX B

GROUND-EFFECT TEST RIG DESIGN

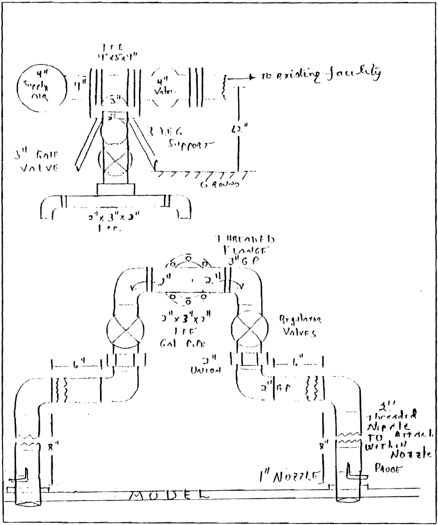

Figure 32. Ground-Effect Test Rig Design

APPENDIX C

GANTRY CRANE WITH MODEL SUSPENSION SYSTEM

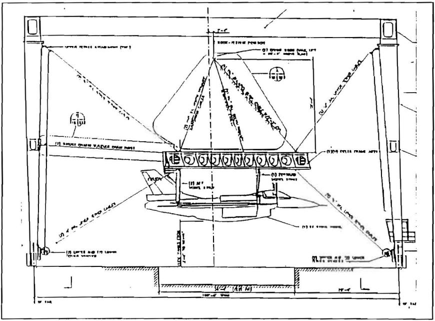

Figure 32. NASA Ames OARF Suspension System

APPENDIX D

PROPOSED MODEL SUPPORT SYSTEM (STRUT CONFIGURATION 2)

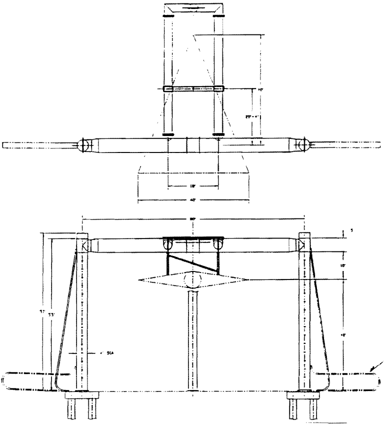

Figure 33. CALF Overhead Support Double Tee Frame Concept

APPENDIX E

NOZZLE PRESSURE RATIO CALCULATIONS

T	Thrust	A	Area
$\dot{m}$	Mass Flow Rate	ρ	Density
V	Velocity	M	Mach
P_e	Exit Pressure	a	Speed of Sound $a=(\gamma RT)^{1/2}$
P_a	Ambient Pressure	D	Diameter (inches)
P_t	Stagnation Pres (psi)		
R	Gas Constant	t	Temperature

T_A/T_F Thrust Aft Nozzle/Thrust Forward Nozzle (Thrust Ratio)

THRUST EQUATION $T = \dot{m}V + (P_e - P_a)A$

For underexpanded nozzle $P_e = P_a$

$$T = \dot{m}V = \rho AV^2 = (P_e/Rt)A(aM)^2 = (P_e/Rt)A(\gamma RT)M^2 = P_e A\gamma M^2$$

NPR I (THRUST RATIO .67)

NOZZLE	NPR	D	P_t	M
Forward	1.624	1.0	23.9	.863
Aft	1.323	1.1	19.4	.642

$$T_A/T_F = (P_e A\gamma M^2)_A/(P_e A\gamma M^2)_F = (D^2M^2)_A/(D^2M^2)_F$$

$$T_A/T_F = (1.1)^2(.642)^2/(.863)^2 = .67$$

NPR II (THRUST RATIO .8)

NOZZLE	NPR	D	P_t	M
Forward	1.624	1.0	23.9	.863
Aft	1.389	1.1	20.4	.702

$T_A/T_F = (P_e A\gamma M^2)_A/(P_e A\gamma M^2)_F = (D^2M^2)_A/(D^2M^2)_F$

$T_A/T_F = (1.1)^2(.702)^2/(.863)^2 = .8$

NPR III (THRUST RATIO 1.1)

NOZZLE	NPR	D	P_t	M
Forward	1.621	1.0	23.9	.863
Aft	1.560	1.1	22.9	.823

$T_A/T_F = (P_e A\gamma M^2)_A/(P_e A\gamma M^2)_F = (D^2M^2)_A/(D^2M^2)_F$

$T_A/T_F = (1.1)^2(.823)^2/(.863)^2 = 1.1$

APPENDIX F

PHOTOGRAPHIC RECORD OF TEST RUNS

I. NPR I NO STRUTS

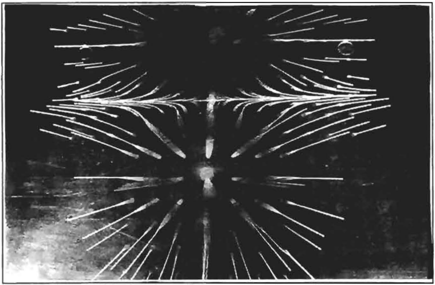

Figure 34. NPR I, Ground-Plane Height 1.5"

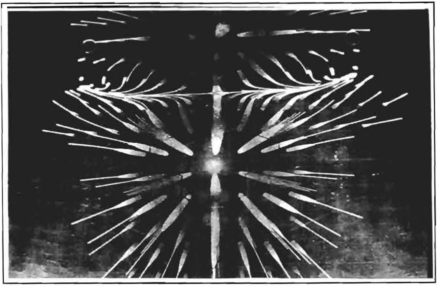

Figure 35. NPR I, Ground-Plane Height 3.0"

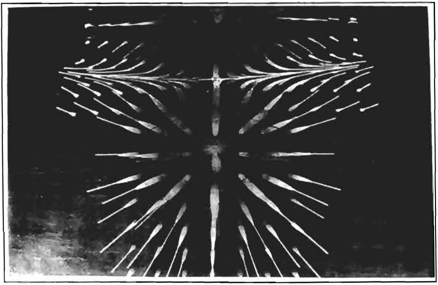

Figure 36. NPR I, Ground-Plane Height 6.0"

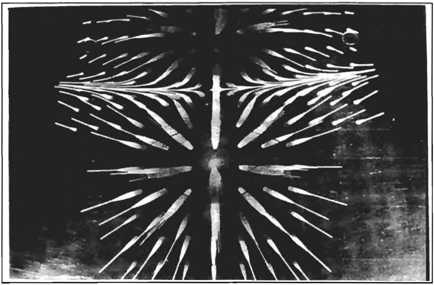

Figure 37. NPR I, Ground-Plane Height 9.0"

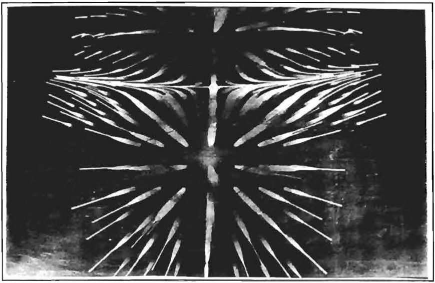

Figure 38. NPR I, Ground-Plane Height 12.0"

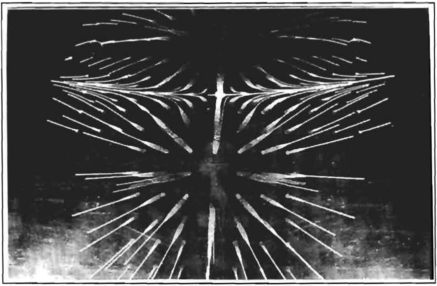

Figure 39. NPR I, Ground-Plane Height 15"

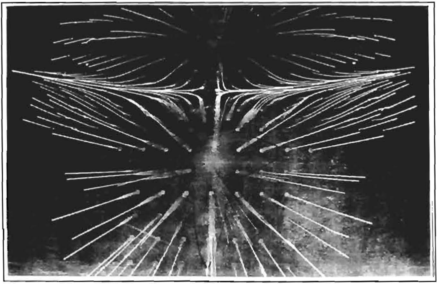

Figure 40. NPR I, Ground-Plane Height 22.25"

II. NPR I STRUT CONFIGURATION 1

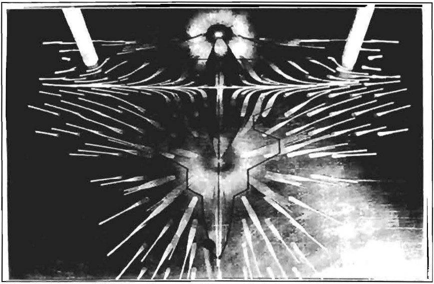

Figure 41. NPR I, Ground-Plane Height 1.5"

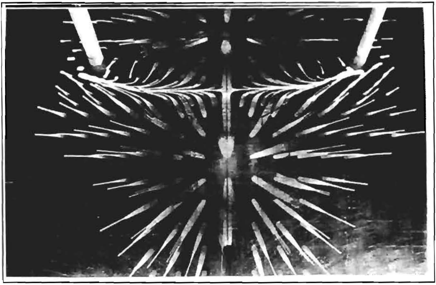

Figure 42. NPR I, Ground-Plane Height 3.0"

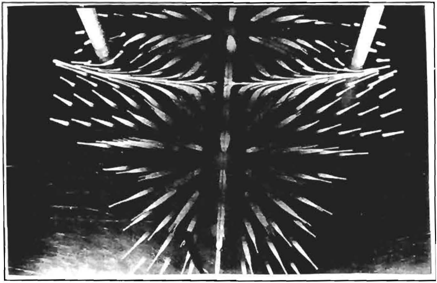

Figure 43. NPR I, Ground-Plane Height 6.0"

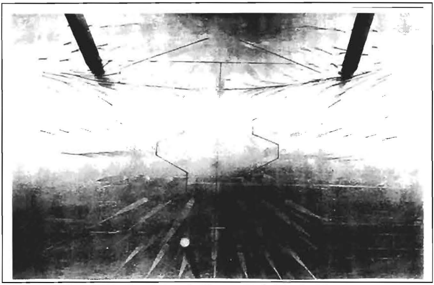

Figure 44. NPR I, Ground-Plane Height 9.0"

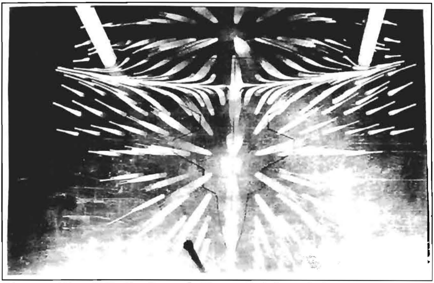

Figure 45. NPR I, Ground-Plane Height 12.0"

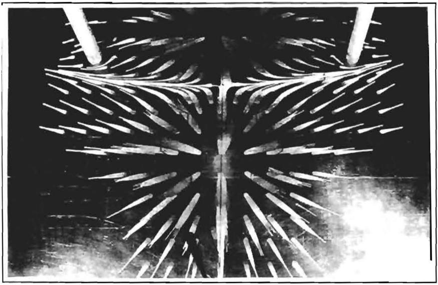

Figure 46. NPR I, Ground-Plane Height 15.0"

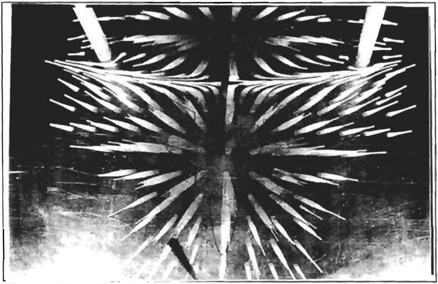

Figure 47. NPR I, Ground-Plane Height 22.5"

III. NPR I STRUT CONFIGURATION 2

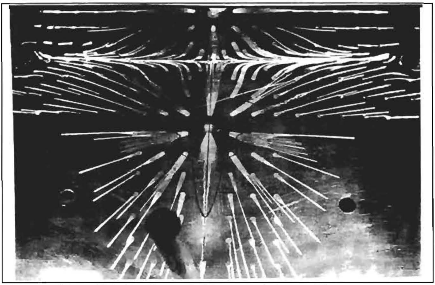

Figure 48. NPR I, Ground-Plane Height 1.5"

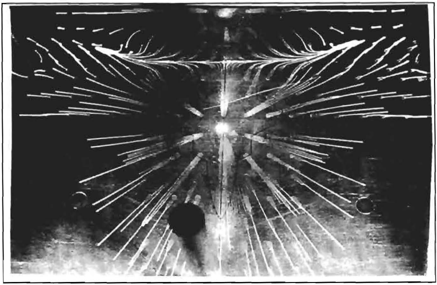

Figure 49. NPR I, Ground-Plane Height 3.0"

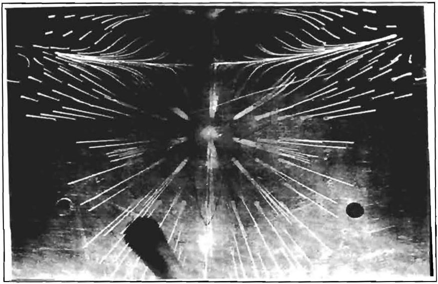

Figure 50. NPR I, Ground-Plane Height 6.0"

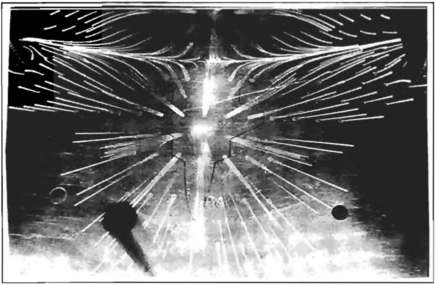

Figure 51. NPR I, Ground-Plane Height 9.0"

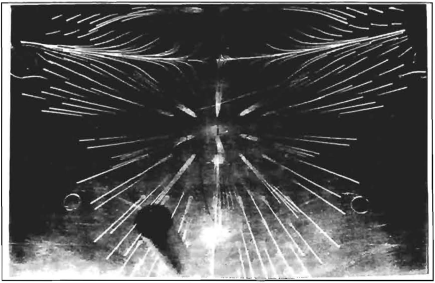

Figure 52. NPR I, Ground-Plane Height 12.0"

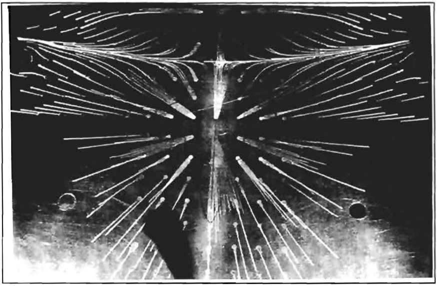

Figure 53. NPR I, Ground-Plane Height 15.0"

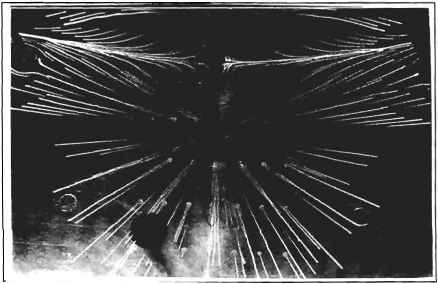

Figure 54. NPR I, Ground-Plane Height 22.25"

IV. NPR II NO STRUTS

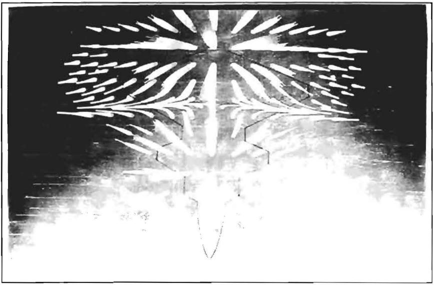

Figure 55. NPR II, Ground-Plane Height 1.5"

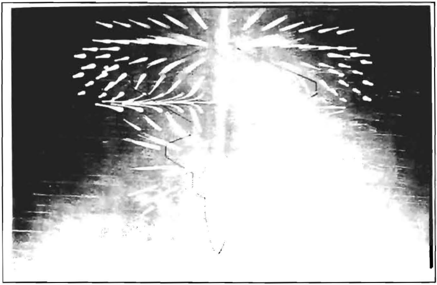

Figure 56. NPR II, Ground-Plane Height 3.0"

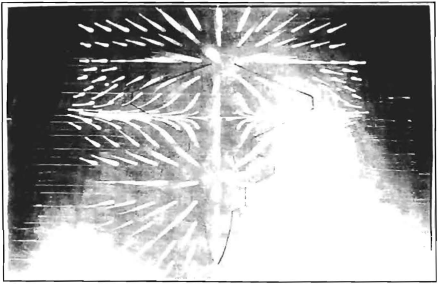

Figure 57. NPR II, Ground-Plane Height 6.0"

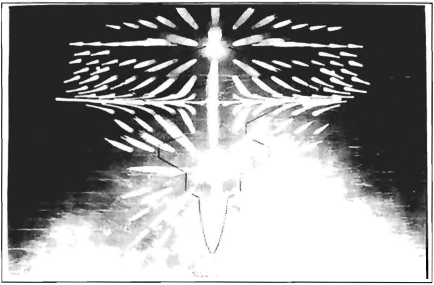

Figure 58. NPR II, Ground-Plane Height 9.0"

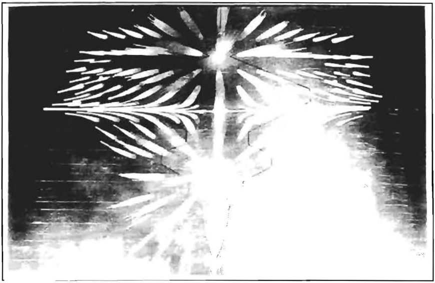

Figure 59. NPR II, Ground-Plane Height 12.0"

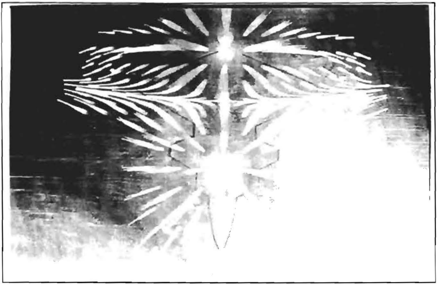

Figure 60. NPR II, Ground-Plane Height 15.0"

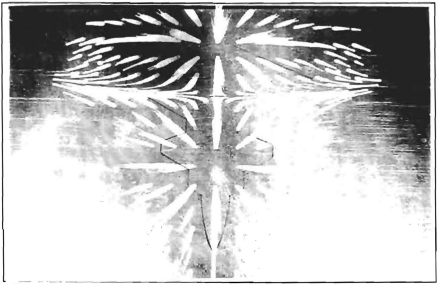

Figure 61. NPR II, Ground-Plane Height 22.25"

V. NPR II STRUT CONFIGURATION 1

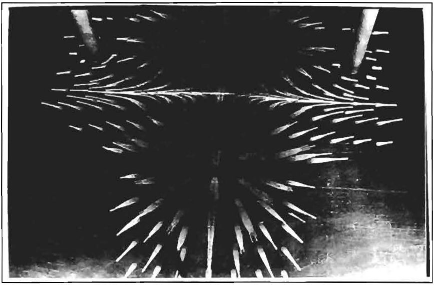

Figure 62. NPR II, Ground-Plane Height 1.5"

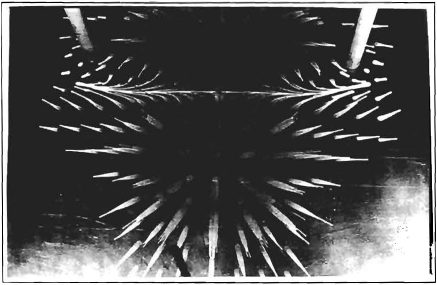

Figure 63. NPR II, Ground-Plane Height 3.0"

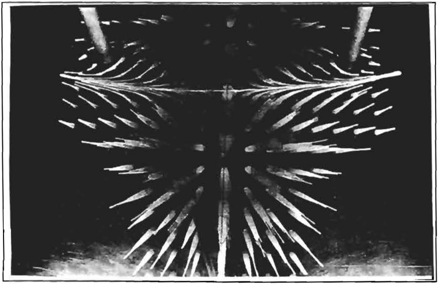

Figure 64. NPR II, Ground-Plane Height 6.0"

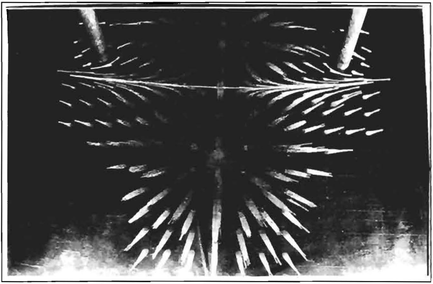

Figure 65. NPR II, Ground-Plane Height 9.0"

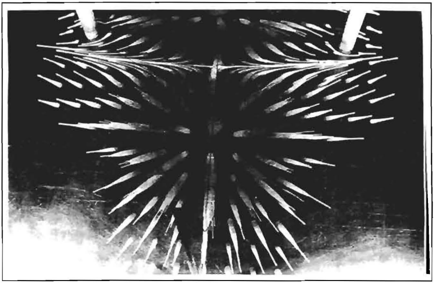

Figure 66. NPR II, Ground-Plane Height 12.0"

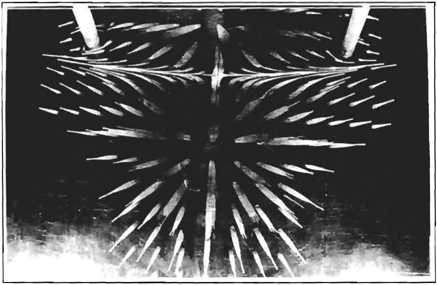

Figure 67. NPR II, Ground-Plane Height 15.0"

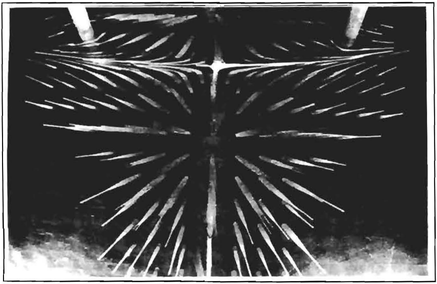

Figure 68. NPR II, Ground-Plane Height 22.25"

VI. NPR III NO STRUTS

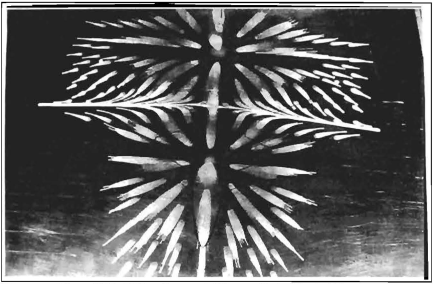

Figure 69. NPR III, Ground-Plane Height 1.5"

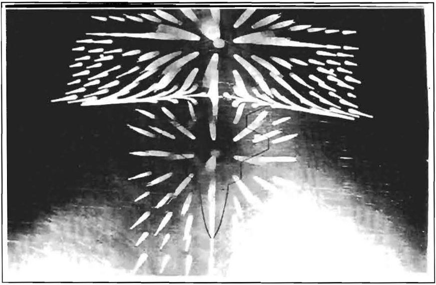

Figure 70. NPR III, Ground-Plane Height 3.0"

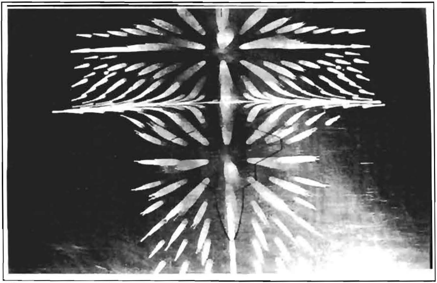

Figure 71. NPR III, Ground-Plane Height 6.0"

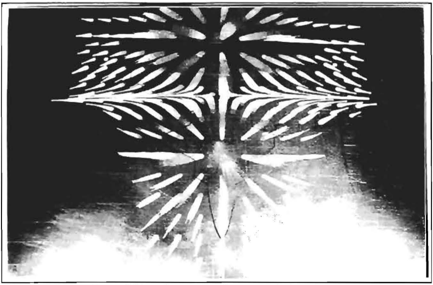

Figure 72. NPR III, Ground-Plane Height 9.0"

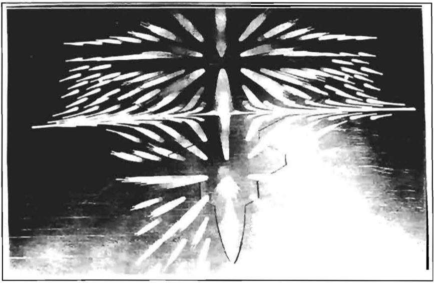

Figure 73. NPR III, Ground-Plane Height 12.0"

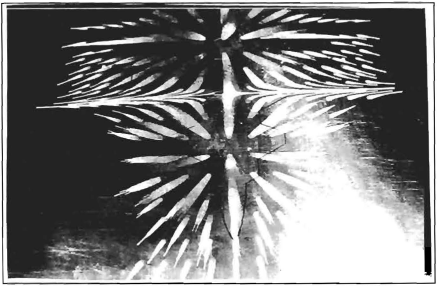

Figure 74. NPR III, Ground-Plane Height 15.0"

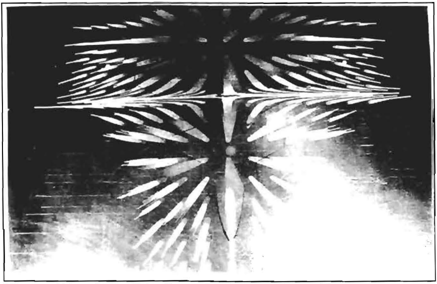

Figure 75. NPR III, Ground-Plane Height 22.25"

VII. NPR III STRUT CONFIGURATION 1

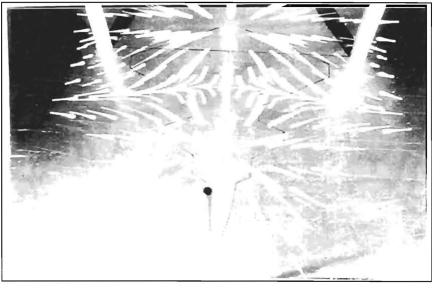

Figure 76. NPR III, Ground-Plane Height 1.5"

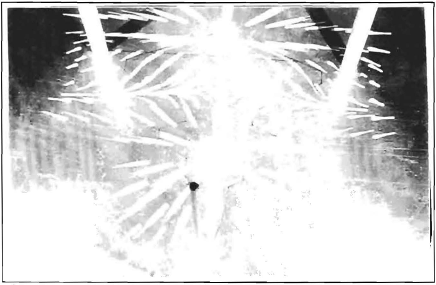

Figure 77. NPR III, Ground-Plane Height 3.0"

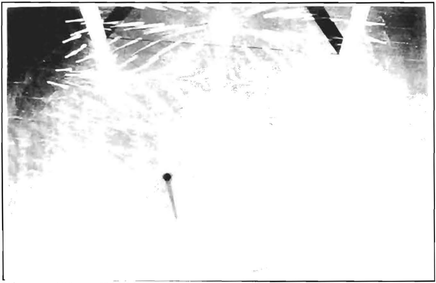

Figure 78. NPR III, Ground-Plane Height 6.0"

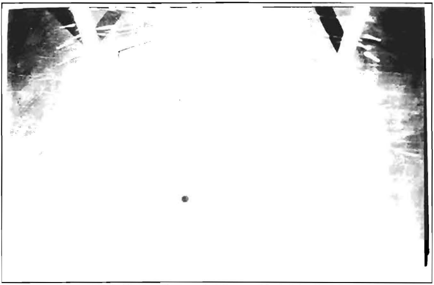

Figure 79. NPR III, Ground-Plane Height 9.0"

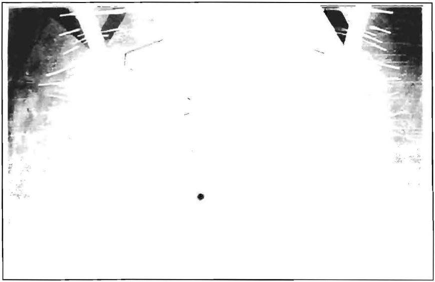

Figure 80. NPR III, Ground-Plane Height 12.0"

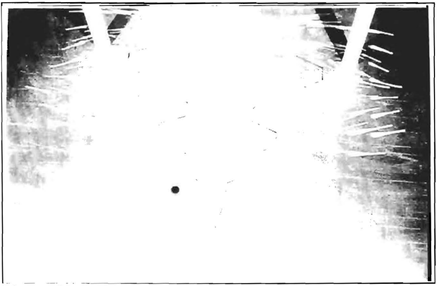

Figure 81. NPR III, Ground-Plane Height 15.0"

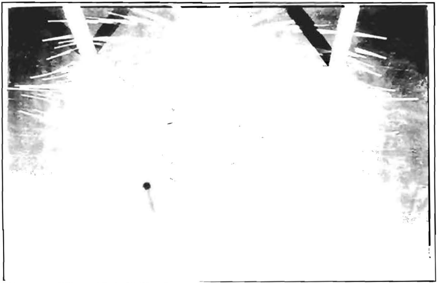

Figure 82. NPR III, Ground-Plane Height 22.25"

VIII. NPR III STRUT CONFIGURATION 2

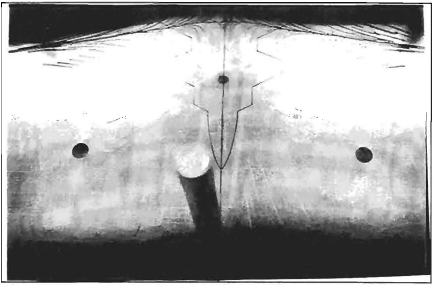

Figure 83. NPR III, Ground-Plane Height 1.5"

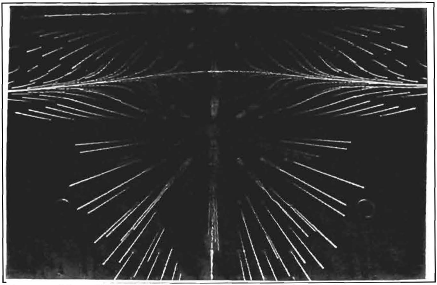

Figure 84. NPR III, Ground-Plane Height 3.0"

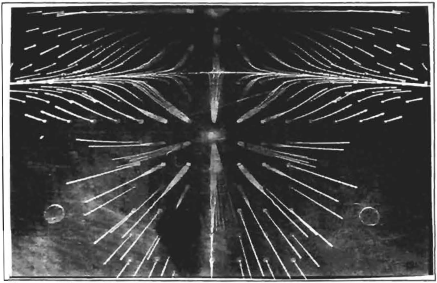

Figure 85. NPR III, Ground-Plane Height 6.0"

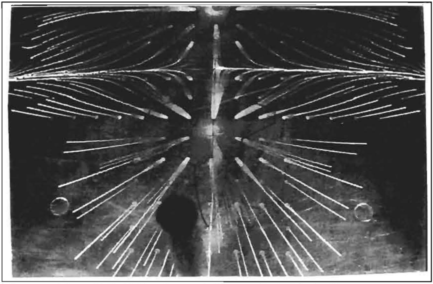

Figure 86. NPR III, Ground-Plane Height 9.0"

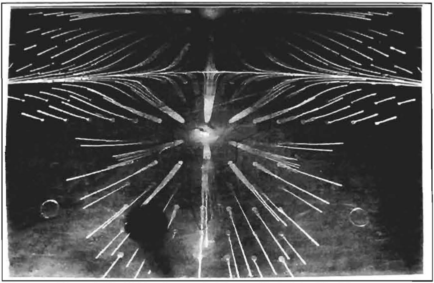

Figure 87. NPR III, Ground-Plane Height 12.0"

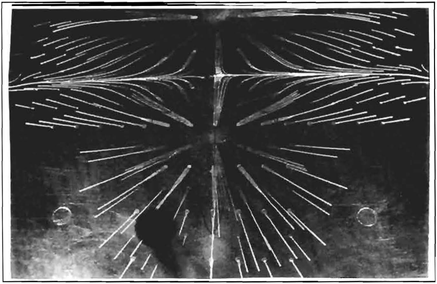

Figure 88. NPR III, Ground-Plane Height 15.0"

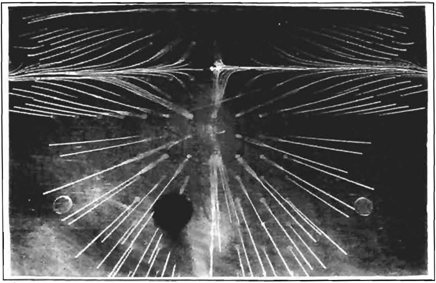

Figure 89. NPR III, Ground-Plane Height 22.25"

APPENDIX G

EXPERIMENTAL RESULTS

TABLE 1: NPR I NO STRUTS STAGNATION LINE MEASUREMENTS (RUN 1)

HEIGHT	1.5	3.0	6.0	9.0	12.0	15.0	22.25
NOSE	15.75	15.56	15.69	15.94	16.00	15.94	15.94
LWING	1.50	1.50	0.00	-0.50	-0.13	-0.19	-0.25
RWING	1.75	2.25	1.50	0.63	0.00	0.75	0.88
LSTRUT	3.25	1.75	2.00	1.38	1.63	1.56	1.63
RSTRUT	3.38	2.38	2.75	2.25	1.75	2.38	2.44

(ALL MEASUREMENTS IN INCHES)

TABLE 2: NPR I NO STRUTS STAGNATION LINE MEASUREMENTS (RUN 2)

HEIGHT	1.5	3.0	6.0	9.0	12.0	15.0	22.25
NOSE	15.88	15.81	15.81	16.00	16.06	16.00	16.13
LWING	1.75	1.75	0.31	-0.13	-0.13	0.00	-0.25
RWING	1.81	2.00	1.13	0.81	0.25	0.63	0.63
LSTRUT	3.06	1.94	2.13	1.81	1.69	1.94	1.75
RSTRUT	3.13	2.25	2.56	2.31	2.13	2.13	2.19

(ALL MEASUREMENTS IN INCHES)

TABLE 3: NPR II NO STRUTS STAGNATION LINE MEASUREMENTS

HEIGHT	1.5	3.0	6.0	9.0	12.0	15.0	22.25
NOSE	15.56	15.38	15.31	15.38	15.63	15.75	15.75
LWING	3.00	3.13	1.56	1.63	0.94	0.50	0.38
RWING	3.19	3.25	2.75	2.63	2.19	1.50	2.00
LSTRUT	4.13	3.50	2.88	3.00	2.44	2.31	2.19
RSTRUT	4.19	3.88	3.25	3.56	3.19	2.88	3.00

(ALL MEASUREMENTS IN INCHES)

TABLE 4: NPR III NO STRUTS STAGNATION LINE MEASUREMENTS

HEIGHT	1.5	3.0	6.0	9.0	12.0	15.0	22.25
NOSE	14.88	14.81	15.00	15.06	15.06	15.12	15.94
LWING	4.88	4.69	3.88	3.75	3.69	3.62	3.75
RWING	4.94	4.56	3.88	3.88	3.56	3.38	3.00
LSTRUT	6.19	5.69	4.94	4.69	4.56	4.50	4.63
RSTRUT	6.06	5.63	4.88	4.69	4.38	4.19	4.13

(ALL MEASUREMENTS IN INCHES)

TABLE 5: NPR I STRUT CONFIGURATION 1 MEASUREMENTS

HEIGHT	1.5	3.0	6.0	9.0	12.0	15.0	22.25
NOSE	15.88	15.88	16.06	16.06	16.13	16.13	16.13
LWING	1.00	-0.75	-0.50	-0.69	-0.44	-0.50	-0.69
RWING	1.75	1.50	1.00	0.75	0.00	0.34	0.00
LSTRUT	2.50	1.34	1.50	1.34	1.56	1.62	1.50
RSTRUT	2.75	2.00	2.50	2.13	1.88	2.25	1.88

(ALL MEASUREMENTS IN INCHES)

TABLE 6: NPR II STRUT CONFIGURATION 1 MEASUREMENTS

HEIGHT	1.5	3.0	6.0	9.0	12.0	15.0	22.25
NOSE	15.63	15.56	15.50	15.75	15.88	15.88	15.88
LWING	2.63	2.38	0.75	1.00	0.00	0.13	0.00
RWING	2.75	2.81	2.25	1.50	1.31	1.50	1.63
LSTRUT	3.94	2.69	2.25	2.50	1.88	2.00	1.94
RSTRUT	3.88	3.31	3.00	2.63	2.56	2.69	2.81

(ALL MEASUREMENTS IN INCHES)

TABLE 7: NPR III STRUT CONFIGURATION 1 MEASUREMENTS

HEIGHT	1.5	3.0	6.0	9.0	12.0	15.0	22.25
NOSE	15.13	14.88	15.00	15.06	15.13	15.25	15.19
LWING	4.19	4.06	3.50	3.13	2.94	2.75	2.88
RWING	4.50	4.38	3.94	3.75	3.56	3.50	3.50
LSTRUT	5.50	5.00	4.31	4.25	3.75	3.56	3.69
RSTRUT	5.56	5.13	4.50	4.44	4.25	4.13	4.19

(ALL MEASUREMENTS IN INCHES)

TABLE 8: NPR I STRUT CONFIGURATION 2 MEASUREMENTS

HEIGHT	1.5	3.0	6.0	9.0	12.0	15.0	22.25
NOSE	15.88	15.81	15.94	16.13	16.13	16.06	16.25
LWING	1.00	-0.13	-0.19	-0.56	-0.50	-0.38	-0.38
RWING	1.25	1.31	0.75	0.00	-0.06	0.25	-0.13

(ALL MEASUREMENTS IN INCHES)

TABLE 9: NPR III STRUT CONFIGURATION 2 MEASUREMENTS

HEIGHT	1.5	3.0	6.0	9.0	12.0	15.0	22.25
NOSE	15.06	14.88	15.00	15.00	15.06	15.13	15.06
LWING	4.88	4.50	4.00	3.88	3.88	3.50	3.69
RWING	4.81	4.50	4.13	4.13	3.69	3.63	3.75

(ALL MEASUREMENTS IN INCHES)

APPENDIX H

OPERATING INSTRUCTIONS

I. Supply Air

- A. Ensure all valves are secured.
- B. Inform lab personnel that the air supply will be turned on.
- C. Energize Motor Operated Valve (MOV) circuit breaker.
- D. Activate MOV open switch and observe green light. The red light remains on while the valve is moving. When the red light extinguishes the valve is fully open.
- E. Check pressure gage for available pressure.

II. NPR Selection

- A. Lower ground plane away from the nozzles.
- B. Set the calibration markers on the P1/P2 pressure gages.
- C. Ensure all lab personnel have appropriate hearing protection.
- D. Open main shut-off valve.
- E. Adjust NPRs with individual nozzle pressure regulator valve.
- F. Secure air with main shut-off valve.

III. Ground-Plane Preparation

- A. Clean ground plane with paint thinner solution.
- B. Trace outline of model on ground plane.
- C. Lower ground plane for oil dot application.
    1. Place oil dot template on ground plane.
    2. Apply oil dots with small squeeze bottle applicator.
    3. Remove template and apply additional oil dots in the region of interest.
- D. Raise ground plane to model height to ensure alignment of traced outline is still valid.

IV. Setting Ground-Plane Height

- A. Lower ground plane to desired height.
- B. Measure distance to ground plane at both wingtips, canard tips and nose to ensure level jet exit plane.
- C. Apply wedges as necessary to obtain level ground plane.

V. Performing Jet Nozzle Test Run

- A. Ensure all lab personnel have appropriate hearing protection.
- B. Open main shut-off valve.
- C. Monitor pressure gages and adjust as necessary.
- D. Secure main shut-off valve when oil has dispersed to desired limits. (Approximately five minutes.)

VI. Data Collection and Photography

A. Measure ground-plane height to ensure hydraulic lift has maintained a constant height.

B. Lower ground plane and take required photographs.

C. Take measurements utilizing traced outline of model.

VII. Additional Runs

A. Check supply-air pressure to ensure sufficient air remains for next run.

B. Repeat instructions II to VI for additional runs.

VIII. Securing Supply Air

A. Inform lab personnel that the supply air will be secured.

B. Activate close switch for the MOV. Observe red light while valve is closing. The green light extinguishes when the valve is completely closed.

C. Secure MOV circuit breaker.

D. Ensure lab personnel have appropriate hearing protection.

E. Purge system by opening main shut-off valve.

F. Close main shut-off valve when air flow stops.

APPENDIX I

ASYMMETRY OF GROUND-PLANE FLOW FIELD

A. DESCRIPTION

Due to the symmetric construction of the model it was expected that the ground stagnation line would be symmetric with respect to the nose-to-tail bisection line. A close examination of the photographs (Appendix F) and the measurements (Tables 1-9) reveals an asymmetric pattern to the ground-plane flow field. A quantitative assessment of this asymmetry can be made by comparing the plots of $b\sin\theta$ versus h/D_e for the left and right wings. The asymmetric effect observed for NPR I is displayed in Figures 90-92. It should be noted that the asymmetry was present for all NPR's, with and without struts, and for all h/D_e.

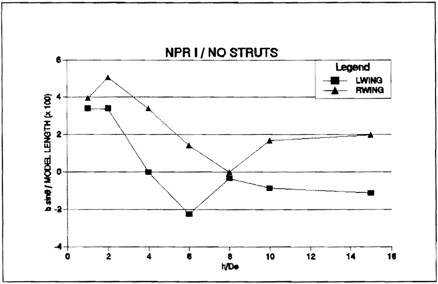

Figure 90. Stagnation Line Asymmetry for NPR I / No Struts

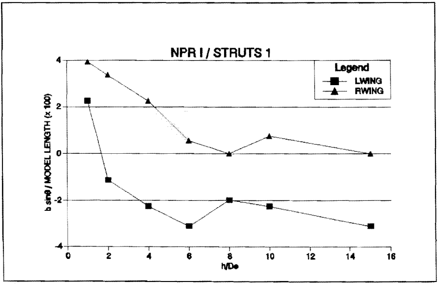

Figure 91. Stagnation Line Asymmetry for NPR I / Struts 1

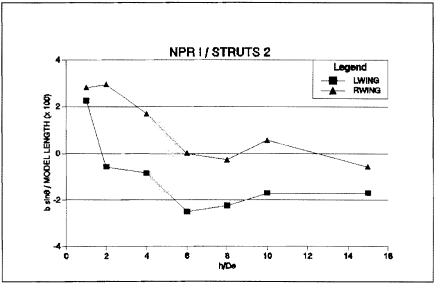

Figure 92. Stagnation Line Asymmetry for NPR II/ Struts 2

B. CAUSE

Every effort was made to remove any possible cause of the resulting asymmetry. Initially the following external factors were suspected to cause the asymmetry:

1. Lift Mechanism

The hydraulic lift mechanism was positioned on three of the four sides of the ground-plane. The relative position of the hydraulic lift had no apparent effect on the asymmetry of the ground-plane flow field.

2. Ground Plane Border

The ground plane initially included a one-inch vertical border that was designed to contain the flow of oil. This border was 23 inches from the centerline of the 46 inch square test bed. The removal of the border had no effect on the asymmetry of the ground-plane flow field.

3. Nozzle Exit Plane

To ensure that the nozzle exit plane was in fact parallel to the ground plane measurements were taken on both sides of the wingtips and the canards. These measurements were taken before and after the test run to ensure that the exit plane remained parallel to the ground plane.

4. Model Reference

The model was traced on the ground plane prior to each run. To ensure that the traced outline remained aligned with the model when the ground plane was lowered a plumb line was used from the corners of each wingtip and canard. No misalignment was detected due to the lowering of the ground plane.

By systematically eliminating the external cause factors the asymmetric flow field was attributed to the internal flow of the supply air. While no attempt was made to isolate the cause factor it was suspected that the design of the supply air piping with its multiple 90° bends, valves, reducers, etc.

introduced an undesirable swirl to the jet nozzles that manifested itself in the asymmetric nature of the ground-plane flow field. Since this asymmetry was present for all runs it effectively resulted in different nozzle exhaust characteristics for the left and right sides of the model. The results are acceptable as long as comparisons are made only between the left or the right side of the model. Note that the effect of asymmetry on the stagnation point itself is minimal.

LIST OF REFERENCES

1. Kandebo, S.W., "NASA Tests Defining ASTOVL Flow Field," *Aviation Week & Space Technology*, v.139, no.13, pp.40-42, 27 September 1993.

2. NASA Ames Research Center Library, Photographs provided by Lockheed Advanced Development Company and McDonnell Douglas, 1994.

3. Levin, D.B. and Wardwell, D.A., "An Experimental Investigation of the Anomalies in Single Jet Suckdown Data," NASA Ames Research Center, 1994 (Unpublished).

4. Winston, M.M., Albang, L.F. and Gentry, G.L., Jr., "*A Simplified Approach for Preliminary Estimation of VTOL Induced Effects in Hover,*" paper presented at the Navy Workshop on Prediction Methods for Jet/VSTOL Propulsion Aerodynamics, Washington D.C., 28 July 1975.

5. Ing, D.N. and Zhang, X., "An Experimental and Numerical Study of Single Jet Impingement Ground-Effect Lift Loss," paper presented at the 1993 AIAA International Powered Lift Conference, Santa Clara, CA, 3 December 1993.

6. Platzer, M.F. and Margason, R.J., "Prediction Methods for Jet V/STOL Propulsion Aerodynamics," *Journal of Aircraft*, vol. 15, no. 2, pp. 69-77, 2 February 1978.

7. Merzkirch, W., *Flow Visualization*, Second Edition, pp. 82-89, Academic Press, Inc., 1987.

8. Margason, R.J., "CALF Thrust and Effective Velocity Ratio," NASA Ames Research Center, 3 May 1994 (Unpublished).

9. Kotansky, D.R. and Glaze, L.W., "The Effects of Ground Wall-Jet Characteristics on Fountain Upwash Flow Formation and Development," paper presented at the 1981 AIAA 14th Fluid and Plasma Dynamics Conference, Palo Alto, CA 23 June 1981.

INITIAL DISTRIBUTION LIST

		No. Copies
1.	Defense Technical Information Center Cameron Station Alexandria, VA 22304-6145	2
2.	Library, Code 52 Naval Postgraduate School Monterey, CA 93943-5002	2
3.	Chairman, Code AA/Co Naval Postgraduate School Monterey, CA 93943-5106	1
4.	Professor S.K. Hebbar, Code AA/Hb Naval Postgraduate School Monterey, CA 93943-5106	5
5.	Professor M.F. Platzer, Code AA/Pl Naval Postgraduate School Monterey, CA 93943-5106	1
6.	Professor Rick Howard, Code AA/Ho Naval Postgraduate School Monterey, CA 93943-5106	1
7.	William Dooley 656 King's Grant Road Virginia Beach, VA 23452	2
8.	Michael J. Harris Aircraft Division Code Air-931 Naval Air Systems Command Washington, D.C. 20361-9320	1
9.	Rich Margason Code FFF, M.S. 247-2 NASA Ames Research Center Moffett Field, CA 94035-1000	1
10.	Larry Olson Chief, Code FFF, M.S. 247-2 NASA Ames Research Center Moffett Field, CA 94035-1000	1

11. Sam Wilson 1
Manager, STOVL/CALF Project
Code FPP, M.S. 237-2
NASA Ames Research Center
Moffett Field, CA 94035-1000

12. Doug Wardwell 1
Aerodynamics Manager, STOVL/CALF Project
Code FPP, M.S. 237-2
NASA Ames Research Center
Moffett Field, CA 94035-1000

13. Tim Naumowicz 1
Code FFF, M.S. 247-2
NASA Ames Research Center
Moffett Field, CA 94035-1000

14. Craig Hange 1
Code FFF, M.S. 247-2
NASA Ames Research Center
Moffett Field, CA 94035-1000

15. Tom Arledge 1
Code FFF, M.S. 247-2
NASA Ames Research Center
Moffett Field, CA 94035-1000

16. Paul Askins 1
Test Director, STOVL/CALF Project
Code FFN, M.S. 221-5
NASA Ames Research Center
Moffett Field, CA 94035-1000

17. Peter Zell 1
Test Director, STOVL/CALF Project
Code FFN, M.S. 221-5
NASA Ames Research Center
Moffett Field, CA 94035-1000

18. Gavin Botha 1
Test Director, STOVL/CALF Project
Code FFN, M.S. 221-5
NASA Ames Research Center
Moffett Field, CA 94035-1000

DUDLEY KNOX LIBRARY
NAVAL POSTGRADUATE SCHOOL
MONTEREY CA 93943-5101

GAYLORD S

DUDLEY KNOX LIBRARY
3 2768 00101530 8